arXiv:1408.4306v1 [astro-ph.EP] 19 Aug 2014

RESEARCH

Effect of lift force on the aerodynamics of dust grains in the protoplanetary disk

Masaki S Yamaguchi[1*] and Shigeo S Kimura[2]

Abstract

We newly introduce *lift force* into the aerodynamics of dust grains in the protoplanetary disk. Although many authors have so far investigated the effects of the drag force, gravitational force and electric force on the dust grains, the lift force has never been considered as a force exerted on the dust grains in the gas disk. If the grains are spinning and moving in the fluid, then the lift force is exerted on them. We show in this paper that the dust grains can be continuously spinning due to the frequent collisions so that the lift force continues to be exerted on them, which is valid in a certain parameter space where the grain size is larger than ~ 1 m and where the distance from the central star is larger than 1 AU for the minimum mass solar nebula. In addition, we estimate the effects of the force on the grain motion and obtain the result that the mean relative velocity between the grains due to the lift force is comparable to the gas velocity in the Kepler rotational frame when the Stokes number and lift-drag ratio are both ~ 1. This estimation is performed under the assumptions of the steady state and the isotropic spin angular momentum. We also estimate the mean relative velocity when the grains keep spinning and conclude that the lift force marginally affects the mean relative velocity in the minimum mass solar nebula. If there is a grain-concentrated part in the disk, the relative velocity due to the lift force may dominate there because of high collision rate.

Keywords: gas disk: protoplanetary; aerodynamics: dust grains

1 Background

In the theory of the planet formation, the issue concerning the radial drift of the meter-size dust remains an open question. In the typical scenario μm-size dust grains grow up to be km-size planetesimals via the collision and merging in the protoplanetary disk [7, 9]. When the dust grain grows to be meter-sized, it has a velocity with respect to the disk gas to lose its angular momentum due to the drag force. Thus, the grain falls down to the central star, so that it cannot grow further [1, 4].

Various scenarios are proposed for solving the issue on the meter-size dust. The gravitational instability in the dust layer was investigated at first [7, 16]. In this scenario the dust grains settle toward the mid-plane to form the dense layer, which then fragments into precursors of the planetesimals. However, the sedimentation of the grains leads to the vertical shear of the rotational velocity in the dust layer, which causes the turbulence due to Kelvin-Helmholtz instability. As a result, the grains cannot settle enough to form planetesimals [17]. On the other hand, the effects of turbulence due to magneto-rotational instability were considered [2, 14]. The collision between dust grains occurs more frequently by the increase of the relative velocity due to the turbulence, so that the growth rate of the grains can increase. [4], [10], and [11] have taken into account these effects of the turbulence, and while the first one has found that the dust grains fall down to the central star if the grain density is relatively large, the second and third ones have found that the dust grains can grow sufficiently rapidly to avoid the issue of the meter-size dust when the grains are fluffy. As another scenario [22] has suggested, the planetesimals are formed by the streaming instability caused by the interaction between the dust grains and disk gas.

We newly introduce *lift force* as a factor affecting the relative velocity between the dust grains. When a grain moves in fluid and when the fluid around the grain has a circulation, the lift force is exerted on the grain perpendicularly to the grain velocity, generally

*Correspondence: masaki.yamaguchi@nao.ac.jp
[1]National Astronomical Observatory, 2-21-1 Osawa, Mitaka, Tokyo, Japan
Full list of author information is available at the end of the article

represented as,

$$F_{\rm L} = C_{\rm L} \cdot \frac{\pi r_{\rm d}^2}{m_{\rm d}} \cdot \frac{1}{2}\rho_{\rm g}|\vec{u}|^2 \ , \tag{1}$$

where $C_{\rm L}$ and $\vec{u}$ is a coefficient of the lift force and a velocity of a dust grain relative to the disk gas, respectively. We note here that $F_{\rm L}$ is defined as the lift force per unit mass. The coefficient of the lift force is determined by properties of the grain and flow. For a rotating sphere, the lift force is expressed as

$$\vec{F_{\rm L}} = \frac{\pi\rho_{\rm g} r_{\rm d}^3}{m_{\rm d}} \vec{\omega}_{\rm d} \times \vec{u}, \tag{2}$$

where the Stokes law, which is valid when the Reynolds number is small, is adopted as the drag law [13, 20]. In this case, the coefficient of the lift force is represented as

$$C_{\rm L} = \frac{2m_{\rm d}F_{\rm L}}{\pi r_{\rm d}^2 \rho_{\rm g} u^2} = \frac{2r_{\rm d}\omega_{\rm d}}{u}\sin\theta, \tag{3}$$

where θ is the angle between $\vec{\omega}_{\rm d}$ and $\vec{u}$. When the Reynolds number is so large that the turbulent flow is dominated, and when the Knudsen number is so large that the fluid cannot be regarded as a continuum, the lift force has not yet been formulated. Therefore, in this paper, we investigate the effects of the lift force only when Equation (2) can be applied. We estimate the conditions under which the lift force is kept exerted on the grain in Section 2. We derive and reduce an equation of motion for the grain to estimate the relative velocity between the grains in Section 3. In Section 4, we evaluate the relative velocity between the grains when the lift force is kept exerted on the grains and discuss improvement of our model. Finally we summarize our study in Section 5.

2 Sustainability of the spin of the dust grains

In this section, we examine whether the dust grains keep spinning in the gas disk because the lift force does not act on the non-spinning spherical object. Here, we assume that the collisions between the dust grains induce the spin of the dust grains. The spinning dust is subjected to the torque due to the friction by the background viscous fluid. After the spin-down time scale, the spin of the dust would stop. We estimate the collision time $t_{\rm col}$ and the spin-down time $t_{\rm spindown}$. By comparing these timescales, we obtain the parameter space where the lift force can act on the spinning dust grains. These timescales depend on the disk structure. We adopt the parameters for the disk structure in this paper as follows:

$$\Sigma_{\rm g} = \Sigma_0 R_1^{-q}, \tag{4}$$
$$\Sigma_{\rm d} = f_{\rm d}\Sigma_{\rm g} = f_{\rm d}\Sigma_0 R_1^{-q}, \tag{5}$$
$$c_{\rm s} = \sqrt{\frac{kT}{\overline{m}}} = c_{\rm s,0} R_1^{-p}, \tag{6}$$
$$\Omega_{\rm K} = \sqrt{\frac{GM_{\rm s}}{R^3}} = \Omega_0 R_1^{-3/2}, \tag{7}$$
$$v_{\rm K} = R\Omega_{\rm K} = \Omega_0 R_0 R_1^{-1/2}, \tag{8}$$
$$H_{\rm g} = \frac{\sqrt{2}c_{\rm s}}{\Omega_{\rm K}} = \frac{\sqrt{2}c_{\rm s,0}}{\Omega_0} R_1^{-p+3/2}, \tag{9}$$
$$\rho_{\rm g} = \frac{\Sigma_{\rm g}}{\sqrt{\pi}H_{\rm g}} = \frac{\Sigma_0\Omega_0}{\sqrt{2\pi}c_{\rm s,0}} R_1^{p-q-3/2}, \tag{10}$$

where R is the semi-major axis, R_0 is typical radius of the disk, $R_1 = R/R_0$, $f_{\rm d}$ is the dust-to-gas mass ratio, $\overline{m} = 2.35 m_H$ is the mean particle mass of gas, and $M_{\rm s} = 1 M_\odot$ is the mass of the central star. We use the isothermal sound speed $c_{\rm s}$ and the mid-plane gas density $\rho_{\rm g}$ when estimating timescales. If we choose $\Sigma_0 = 1.7 \times 10^3 {\rm g\ cm^{-2}}$, $c_{\rm s,0} = 1.0 \times 10^5 {\rm cm\ sec^{-1}}$, $\Omega_0 = 2.0 \times 10^{-7} {\rm sec^{-1}}$, $R_0 = 1$ AU, $f_{\rm d} = 0.01$, $q = 3/2$, and $p = 1/4$, the disk profile is similar to the minimum mass solar nebula (MMSN, [9]).

2.1 Collision timescale

Collision time scale is estimated as

$$t_{\rm col} \sim (n_{\rm d} \cdot \pi r_{\rm d}^2 \cdot < v_{\rm d\text{-}d} >)^{-1} \ , \tag{11}$$

where $n_{\rm d}$ and $v_{\rm d\text{-}d}$ is the number density of the dust grains and the relative velocity between the dust grains, respectively. The parenthetic quantity $< Q >$ represents the statistical average.

The dust number density is expressed as

$$n_{\rm d} = \frac{\Sigma_{\rm d}}{H_{\rm d} m_{\rm d}}, \tag{12}$$

where $H_{\rm d}$ is the scale height of the dust layer, $m_{\rm d}$ is the mass of the dust grains. We approximate that the mass distribution function of the dust is the delta function since it is necessary for the dust grains to collide with the similar scale grains so that the grains gain the angular momentum. Considering the equilibrium between turbulent diffusion and sedimentation [3], $H_{\rm d}$ is obtained as

$$H_{\rm d} = H_{\rm g} \cdot \left(\frac{\alpha}{\rm St}\frac{1+2{\rm St}}{1+{\rm St}^2}\right)^{1/2} \ , \tag{13}$$

where ${\rm St} \equiv \Omega_{\rm K} t_{\rm s}$ is the stokes number ($t_{\rm s}$ is the stopping time by drag force). We use alpha prescription

$\nu_{\rm turb} = \alpha c_{\rm s} H_{\rm g}$ to describe the strength of the turbulence in the protoplanetary disk, and assume $\alpha < {\rm St}$ to avoid the situation $H_{\rm g} < H_{\rm d}$. At the Stokes drag law regime, the Stokes number is written as

$$ {\rm St} = \frac{m_{\rm d}\Omega_{\rm K}}{6\pi r_{\rm d}\rho_{\rm g}\nu} = \frac{2\rho_{\rm int} r_{\rm d}^2 \Omega_{\rm K}}{3\rho_{\rm g} c_{\rm s}\lambda_{\rm mfp}} = \frac{2\sigma_{\rm mol}\rho_{\rm int}\Omega_0}{3\overline{m}c_{\rm s,0}} r_{\rm d}^2 R_1^{p-3/2}, \tag{14} $$

where $\rho_{\rm int}$ is the internal mass density of the dust grains, $\nu = c_{\rm s}\lambda_{\rm mfp}/3$ is the kinematic viscosity, $\lambda_{\rm mfp}$ is the mean free path of the gas particles. The mean free path is estimated as $\lambda_{\rm mfp} = \overline{m}/(\sigma_{\rm mol}\rho_{\rm g})$, where $\sigma_{\rm mol}$ is the cross section of collisions between H_2 molecules. We adopt $\rho_{\rm int} \simeq 3$ g cm^{-3}, and $\sigma_{\rm mol} \simeq 2\times10^{-15}$ cm^2. Equation (14) means that the Stokes number is independent of the normalization coefficient of the surface density Σ_0, which is canceled out due to the one in $\lambda_{\rm mfp}$.

Since the gas was assumed to be in a turbulent state described by the alpha prescription, we set the mean relative velocity $< v_{\rm d\text{-}d} > = < v_{\rm d\text{-}d} >_t$, where $< v_{\rm d\text{-}d} >_t$ means the relative velocity between the grains in the turbulent gas. According to [12], $< v_{\rm d\text{-}d} >_t$ with similar scale grains can be represented as

$$ < v_{\rm d\text{-}d} >_t = c_{\rm s}\left(\frac{\alpha {\rm St}}{\sqrt{1+\frac{1}{4}{\rm St}^2(1+{\rm St})^2}}\right)^{1/2}, \tag{15} $$

where we smoothly interpolate the two limiting solutions of ${\rm St} \gg 1$ and ${\rm St} \ll 1$. This expression is valid when the stopping time is larger than the turn-over time of the Kolmogorov-scale eddy. The minimum size of the grain satisfying this condition is on the order of sub-mm for MMSN at 1 AU, so that we focus on the grain larger than ~ 1 mm in what follows.

Now we can express $t_{\rm col}$ as the function of $r_{\rm d}$ and R_1 by using Equations (11) to (15) as

$$ t_{\rm col} = \frac{4\sqrt{2}\rho_{\rm int}}{3\Omega_0\Sigma_0 f_{\rm d}} r_{\rm d} R_1^{q+3/2} f({\rm St}), \tag{16} $$

where

$$ f({\rm St}) = \frac{1}{\rm St}\left(\frac{1+2{\rm St}}{1+{\rm St}^2}\right)^{1/2}\left(1+\frac{1}{4}{\rm St}^2(1+{\rm St})^2\right)^{1/4}. \tag{17} $$

We note that when $\alpha < {\rm St}$, $t_{\rm col}$ is independent of α because the effect increasing $< v_{\rm d\text{-}d} >_t$ balances the one decreasing $n_{\rm d}$. For the case with ${\rm St} \ll 1$, the collision time scale $t_{\rm col} \propto {\rm St}^{-1} r_{\rm d}^1 R_1^{q+3/2} \propto r_{\rm d}^{-1} R_1^{3+q-p}$, while $t_{\rm col} \propto {\rm St}^{-1/2} r_{\rm d}^1 R_1^{q+3/2} \propto r_{\rm d}^0 R_1^{2.25+q-0.5p}$ for the case with ${\rm St} \gg 1$. If we adopt the same parameters as MMSN, collision time is

$$ t_{\rm col} = 1.7\times10^6 f({\rm St}) R_1^3 r_{\rm d,1} \ {\rm sec}, \tag{18} $$

where $r_{\rm d,1} = r_{\rm d}/(1{\rm cm})$.

2.2 Spin-down timescale

In the case of the Stokes law, the angular momentum conservation around the spin axis of a spherical grain is given as

$$ I_{\rm d}\frac{d\omega_{\rm d}}{dt} = -8\pi\rho_{\rm g}\nu r_{\rm d}^3\omega_{\rm d}, \tag{19} $$

where $I_{\rm d}$ is the moment of inertia of the grain. The torque acting onto a spherical body by viscous fluid is given in [13, 20]. From this equation, the $t_{\rm spindown}$ is estimated as

$$ t_{\rm spindown} = \frac{I_{\rm d}}{8\pi\rho_{\rm g}\nu r_{\rm d}^3} = \frac{\rho_{\rm int} r_{\rm d}^2}{5\rho_{\rm g} c_{\rm s}\lambda_{\rm mfp}} = \frac{\sigma_{\rm mol}\rho_{\rm int}}{5\overline{m}c_{\rm s,0}} r_{\rm d}^2 R_1^p. \tag{20} $$

At the second equation, we assume a spherical and uniform density grain whose moment of inertia is represented $I_{\rm d} = 2m_{\rm d}r_{\rm d}^2/5$. The spin-down time becomes longer as the dust grain becomes larger. Here we note that the spin-down time is independent of Σ_0 by the same reason as the Stokes number (see Equation 14). For MMSN, $t_{\rm spindown}$ is estimated as

$$ t_{\rm spindown} = 3.0\times10^3 r_{\rm d,1}^2 R_1^{1/4} {\rm sec}. \tag{21} $$

2.3 Comparison of timescales

Now, we can obtain the size of dust grains that are able to keep spinning. We estimate these time scales just in the Stokes law regime, because the lift force in other regime is uncertain. There are two necessary conditions to realize the Stokes law. One is that the gas can be regarded as a continuum medium, which is expressed as $r_{\rm d} \gtrsim 9\lambda_{\rm mfp}/4$. The other is that the flow around the dust grains is laminar, which is represented as ${\rm Re} = 2ur_{\rm d}/\nu \lesssim 20$ [18], where u is the relative velocity of the dust to the gas. Here, we should actually include the effect of turbulence into the expression of u as in [12] so that the physical situation is consistent with that of Equation (15). However, taking into account the effect causes complicated equations. Thus, as a first-step study, we assume that u is equal to the relative velocity between the orbital velocity of the gas and the Keplerian velocity, i.e., $u = \eta v_{\rm K}$, where

$$ \eta \equiv \frac{2p+2q+3}{4}\left(\frac{c_{\rm s}}{v_{\rm K}}\right)^2, \tag{22} $$

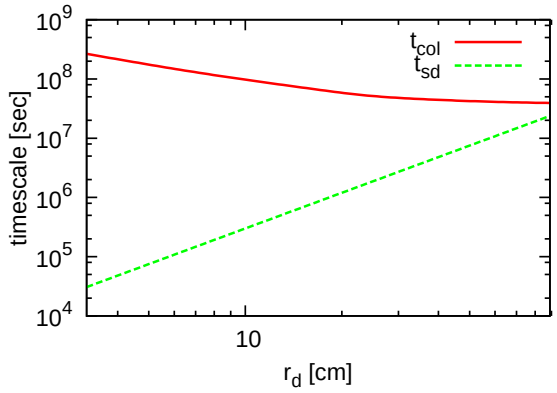

Figure 1 $r_{\rm d}$ dependence of $t_{\rm col}$ (solid lines) and $t_{\rm spindown}$ (dashed lines) at $R_1 = 1$. $t_{\rm col}$ is always longer than $t_{\rm spindown}$ in the Stokes regime.

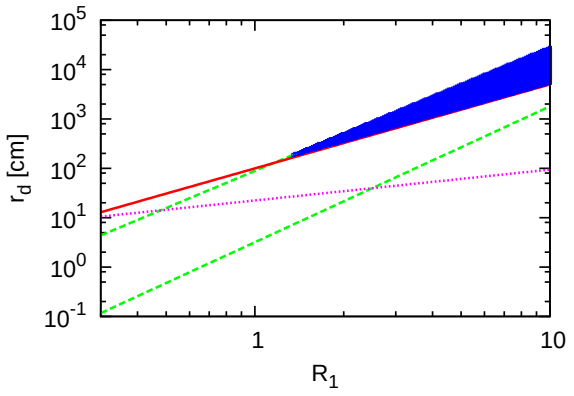

Figure 2 Parameter space where the dust grains can keep spinning in the $r_{\rm d} - R_1$ plane. The Stokes regime is between the two dashed green lines. The condition $t_{\rm col} < t_{\rm spindown}$ is satisfied above the solid red line. The grains may keep spinning in the blue region. The dotted magenta line represents the line where the condition St$= 1$ is satisfied.

which is given in [1]. By these conditions, we find that our estimation is valid in the range,

$$r_{\rm d,min} \lesssim r_{\rm d} \lesssim r_{\rm d,max}, \text{ where}$$
$$r_{\rm d,min} \equiv \frac{9\overline{m}c_{\rm s,0}}{2\sigma_{\rm mol}\Sigma_0\Omega_0} R_1^{q-p+3/2}, \text{ and} \quad (23)$$
$$r_{\rm d,max} \equiv \frac{40\sqrt{2\pi}\overline{m}R_0}{3(2p+2q+3)\sigma_{\rm mol}\Sigma_0} R_1^{q+1}.$$

For MMSN, this condition is simply written as

$$3.2R_1^{11/4} \lesssim r_{\rm d,1} \lesssim 89R_1^{5/2}. \quad (24)$$

Figure 1 shows that the two timescales $t_{\rm col}$ (solid lines) and $t_{\rm spindown}$ (dashed lines) at $R_1 = 1$ for MMSN. We plotted $t_{\rm col}$ and $t_{\rm spindown}$ in the range, which satisfies the condition (24). From Figure 1, we can see that $t_{\rm col}$ is larger than $t_{\rm spindown}$, so that the spin of the dust would stop at $R_1 = 1$. The difference of two timescales are smaller as the dust grains are larger. Equations (18) and (21) shows that large grains are likely to satisfy the condition $t_{\rm col} < t_{\rm spindown}$. From Equation (24), the Stokes regime can be adopted for the larger dust grains at the outer region of the disk. Thus, we expect that the condition $t_{\rm col} < t_{\rm spindown}$ is satisfied at the outer region $R_1 > 1$. Figure 2 shows the parameter space where the dust grains keep spinning in $R_1 - r_{\rm d}$ plane for MMSN. The Stokes regime is realized between the dashed green lines. The condition $t_{\rm col} < t_{\rm spindown}$ is satisfied above the solid red line. In the blue region, the condition is satisfied with the Stokes regime. There are dust grains that keep spinning with the Stokes regime in $R_1 \gtrsim 1.3$. The grains that can keep spinning have the size $r_{\rm d} \sim r_{\rm d,max}$. The dotted magenta line shows the dust radius when St $= 1$, which is used in Section 4.

3 Relative velocity between the dust grains

In this section, we investigate whether the mean relative velocity is comparable to or greater than the gas velocity in the Kepler rotational frame. Since this gas velocity is comparable to the typical relative velocity between a large grain and a small one compared to one-meter-sized dust, we take it as a reference value. First, we derive the equation of motion for a dust grain assuming that it moves at a terminal velocity. Next we estimate the mean relative velocity by assuming the isotropic distribution for the spin angular momentum.

Here, for simplicity, we assume that the dust grains move on the mid-plane of the disk, which means the z-component of the lift force is assumed to be zero, where z-axis is taken as the disk axis, and we adopt below the cylindrical coordinate. Since the direction of the spin angular momentum can be taken arbitrarily, the lift force can show the z-component. Nevertheless, we neglect the z-component of the velocity to simplify the calculation below.

For the preparation to derive the equation of motion, we express a projected vector of the lift force on the mid-plane in terms of the direction of the spin angular momentum of a dust grain. Since the direction of the lift force is perpendicular to the spin angular momentum and the velocity of the grain with respect to the gas, so that

$$\vec{F}_{\rm L} = A\vec{\omega}_{\rm d} \times \vec{u}, \quad (25)$$

where the coefficient satisfies $A = \frac{\pi \rho_{\rm g} r_{\rm d}^3}{m_{\rm d}}$ (see Section 1). Since z-component of $\vec{u}$ is zero, the lift force vector projected on the mid-plane $\vec{F}_{\rm L,mid}$ is expressed as,

$$\vec{F}_{\rm L,mid} = \vec{F}_{\rm L} \cdot \begin{pmatrix} \vec{e}_r \\ \vec{e}_\theta \end{pmatrix} = A\omega_{\rm d}\mu \begin{pmatrix} -u_\theta \\ u_r \end{pmatrix} \equiv F_{\rm L} \begin{pmatrix} -u_\theta/u \\ u_r/u \end{pmatrix}, \tag{26}$$

where $\vec{e}$ with a subscript and μ represent a unit vector in the direction of the subscript and the cosine of the angle between $\vec{\omega}_{\rm d}$ and the z-axis, respectively. We note here that the $F_{\rm L}$ do not depend on the azimuth angle of the spin angular momentum.

Next, we derive and reduce the equation of motion of the dust grain. Now the forces exerted on the dust grain are the gravitational force of the central star, the drag force and the lift force, so the equation of motion is expressed as,

$$\frac{d\vec{v}}{dt} = -\frac{GM_\odot}{r^2}\vec{e}_r - \vec{F}_{\rm D} + \vec{F}_{\rm L,mid}, \tag{27}$$

where we assume that the mass of the central star is the same as the solar one. As the first step of the reduction of Equation (27), we divide it into two equations for r and θ components. Since the velocity of the disk gas does not have the radial component, the components of the velocity of the dust grain are represented as $(u_r, u_\theta) = (v_r, v_\theta - r\Omega_{\rm g})$, where $\Omega_{\rm g}$ is the orbital angular velocity of the disk gas around the central star. Thus, Equation (27) is expressed as,

$$\frac{dv_r}{dt} - \frac{v_\theta^2}{r} = -\frac{GM_\odot}{r^2} - F_{\rm D}\frac{v_r}{u} - F_{\rm L}\frac{v_\theta - r\Omega_{\rm g}}{u}, \tag{28}$$

$$\frac{dv_\theta}{dt} + \frac{v_r v_\theta}{r} = -F_{\rm D}\frac{v_\theta - r\Omega_{\rm g}}{u} + F_{\rm L}\frac{v_r}{u}. \tag{29}$$

As the second step, we transform this into the coordinate rotating at the angular velocity of the Kepler rotation, that is, $v_\theta = v_{\rm K} + v'_\theta$. As the third step, we assume that the motion of the dust grain is stationary, and that $|v_r|, |v'_\theta| \ll v_{\rm K}$.

This stationary assumption may be invalid taking into account the timescales discussed in Section 2. The stopping time $t_{\rm s}$ is represented as,

$$t_{\rm s} = \frac{m_{\rm d}}{6\pi r_{\rm d}\rho_{\rm g}\nu} \sim 10^4\ r_{\rm d,1}^2 R_1^{1/4} \sim 4\ t_{\rm spindown}. \tag{30}$$

This means that the dust grain stops spinning before moving at the terminal velocity independently of the dust size and the distance from the central star. Thus, as long as the lift force is exerted on the grain, the motion of the grain cannot reach a steady state. Alternatively, the grain motion is considered to be determined by the merger of the parent grains (or scattering by the other grain). Nevertheless, we assume that the grain motion reaches the steady state, as the first stage of this kind of work.

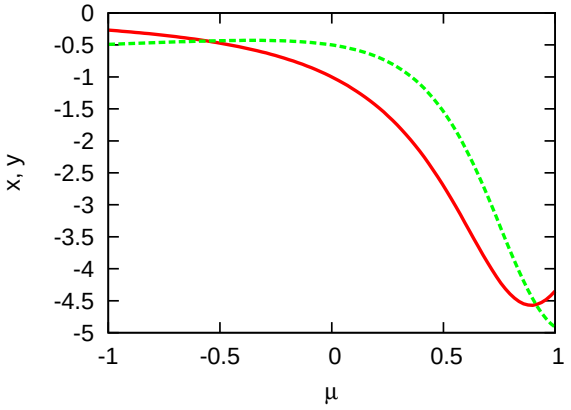

Figure 3 Dependence of the grain velocity in the radial direction x (the solid line) and in the azimuthal direction y (the dashed line) on the cosine of the angle between the spin angular momentum and z-axis μ. We take the parameters as $g_{\rm D} = 1$ and $R_{\rm LD} = 1$.

Finally, we nondimensionalize the variables as

$$x = \frac{v_r}{\eta v_{\rm K}},\ y = \frac{v'_\theta}{\eta v_{\rm K}},\ g_{\rm D} = \frac{F_{\rm D}}{u\Omega_{\rm K}},\ g_{\rm L} = \frac{F_{\rm L}}{u\Omega_{\rm K}}, \tag{31}$$

where η is the constant satisfying the equation $r\Omega_{\rm g} = v_{\rm K}(1-\eta)$, and $\Omega_{\rm K}$ is the angular velocity of the Kepler motion. Thus, we obtain two algebraic equations

$$2y = g_{\rm D}x + g_{\rm L}(y+1), \tag{32}$$

$$\frac{1}{2}x = -g_{\rm D}(y+1) + g_{\rm L}x. \tag{33}$$

These equations represent the balance between Coriolis, drag and lift forces.

The solution of the equations is

$$x = \frac{-2g_{\rm D}}{g_{\rm D}^2 + (g_{\rm L}-2)(g_{\rm L}-1/2)}, \tag{34}$$

$$y = -1 + \frac{-2(g_{\rm L}-1/2)}{g_{\rm D}^2 + (g_{\rm L}-2)(g_{\rm L}-1/2)}. \tag{35}$$

Here, Equations (26) and (31) lead to $g_{\rm L} = g_{\rm L,max}\mu$, where $g_{\rm L,max} \equiv \frac{A\omega_{\rm d}}{\Omega_{\rm g}}$, and we introduce lift-drag ratio $R_{\rm LD} \equiv g_{\rm L,max}/g_{\rm D}$ to obtain $g_{\rm L} = g_{\rm D}R_{\rm LD}\mu$. Thus, x and y are expressed as functions of μ, $g_{\rm D}$ and $R_{\rm LD}$.

We show $x(\mu)$ and $y(\mu)$ in Figure 3. Here we assume $g_{\rm D} = 1$ and $R_{\rm LD} = 1$ as a trial value. Since $x = -1$ when we neglect the lift force, the curve of $x(\mu)$ shows the radial velocity of the dust grain can be a third or four times compared to that without the lift force. On the other hand, when $\mu < 0$, y is almost constant and comparable to that without the lift force. When μ is larger than 0.5, y is smaller than -1, which means that the dust grain orbits more slowly than the gas. In addition, we see that x and y decrease as μ is close to unity. Therefore, the absolute value of the velocity tends to increase as μ increases.

Next, we calculate the average and dispersion of the velocity of the dust grain on the disk mid-plane, assuming that the spin angular momentum is isotropic, which is just for simplicity. Thus, the direction distribution satisfies $f(\Omega) = \frac{1}{4\pi}$, which is equivalent to $f(\mu) = \frac{1}{2}$, where Ω is a solid angle parameter. The average and dispersion of x are calculated by performing the integration below.

$$\begin{aligned} < x > &= \int x f(x) dx \\ &= \frac{1}{2}\int_{-1}^{1} x(\mu) d\mu, \\ < x^2 > &= \int x^2 f(x) dx \\ &= \frac{1}{2}\int_{-1}^{1} x^2(\mu) d\mu, \end{aligned} \tag{36}$$

where we transform the integration variable into μ. We also can derive the same expression for y,

$$\begin{aligned} < y > &= \frac{1}{2}\int_{-1}^{1} y(\mu) d\mu, \\ < y^2 > &= \frac{1}{2}\int_{-1}^{1} y^2(\mu) d\mu. \end{aligned} \tag{37}$$

Taking $g_{\rm D} = 1, R_{\rm LD} = 1$, we obtain the approximate value of the average and standard deviation of the velocity,

$$< x > \simeq -1.4, \tag{38}$$
$$< y > \simeq -1.2, \tag{39}$$
$$\sqrt{< x^2 >} \simeq 1.0, \tag{40}$$
$$\sqrt{< y^2 >} \simeq 0.6, \tag{41}$$
$$< w_{\rm rel} > \equiv \sqrt{< x^2 > + < y^2 >} \simeq 1.2. \tag{42}$$

Equation (38) means that the dust grains averagely fall down to the star faster than without the lift force. On the other hand, Equation (39) means that they averagely orbit at almost the same velocity as the gas.

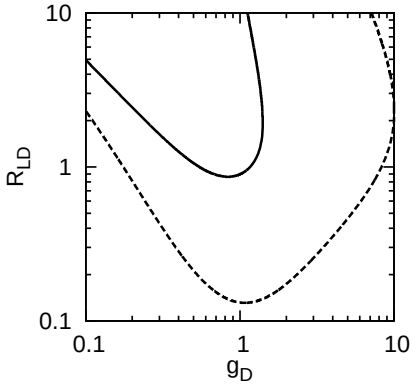

Figure 4 Contours of the averaged relative velocity of the grains are shown on the $g_{\rm D}$-$R_{\rm LD}$ plane. The solid and dashed lines represent $< w_{\rm rel} >= 1$ and 0.1, respectively.

We note that the standard deviation of the velocity represents average of the relative velocity between the grains. Therefore, Equation (42) means that the average relative velocity exceeds the relative velocity between the gas and Kepler velocity, so that the collision rate is affected by the lift force when $g_{\rm D} = 1$ and $R_{\rm LD} = 1$.

We finally calculate the averaged relative velocity on the disk mid-plane $< w_{\rm rel} >$ for arbitrary values of $g_{\rm D}$ and $R_{\rm LD}$. Figure 4 shows the contour lines of $< w_{\rm rel} >=1$ (the solid line) and 0.1 (the dashed line) on the $g_{\rm D}$-$R_{\rm LD}$ plane. We see that the relative velocity is large when $g_{\rm D}$ is small and when $R_{\rm LD}$ is large, which corresponds the situation that the lift force is efficiently exerted on the grains. The important fact is that there exist a region satisfying $< w_{\rm rel} >> 1$, where the lift force non-negligibly affects the dynamics of the system of grains, compared to the case without the force.

4 Discussion

4.1 Lift-drag ratio

In this subsection, we estimate the lift-drag ratio $R_{\rm LD}$ to investigate how efficiently the lift force affects the motion of the dust. In the Stokes regime, the lift coefficient $C_{\rm L}$ and drag coefficient $C_{\rm D}$ is represented as

$$C_{\rm D} = \frac{4 c_{\rm s} \lambda_{\rm mfp}}{r_{\rm d} u}, \tag{43}$$
$$C_{\rm L} = \frac{2 m_{\rm d} F_{\rm L}}{\pi r_{\rm d}^2 \rho_{\rm g} u^2} = \frac{2 r_{\rm d} \omega_{\rm d}}{u} \sin\theta. \tag{44}$$

The lift coefficient depends on the spin angular velocity $\omega_{\rm d}$ of the dust. Here, we estimate $\omega_{\rm d}$ induced

by the collisions of the grains. When two grains with the same mass $m_{\rm d}$ collide with the impact parameter b, the angular momentum around the center of mass is represented by

$$L = \frac{b v_{\rm d\text{-}d} m_{\rm d}}{2}. \tag{45}$$

Given the weight by a cross section, we derive the averaged angular velocity $\sqrt{< L^2 >}$ as

$$\sqrt{< L^2 >} = \left(\frac{\int_0^{2r_{\rm d}} L^2 2\pi b db}{\int_0^{2r_{\rm d}} 2\pi b db} \right)^{1/2} = \frac{1}{\sqrt{2}} < v_{\rm d\text{-}d} > r_{\rm d} m_{\rm d}. \tag{46}$$

If we assume that the grain obtains the mass $2m_{\rm d}$ and this angular momentum after the collision, the resultant angular velocity $\omega_{\rm d}$ is represented as

$$\omega_{\rm d} = \frac{5\sqrt{2}}{4} \frac{< v_{\rm d\text{-}d} >}{r_{\rm d}}. \tag{47}$$

Using Equation (43), (44), and (47), we can reduce the lift-drag ratio $R_{\rm LD}$ as

$$R_{\rm LD} = \frac{C_{\rm L}}{C_{\rm D}} = \frac{5\sqrt{2} r_{\rm d} < v_{\rm d\text{-}d} >}{8 c_{\rm s} \lambda_{\rm mfp}}. \tag{48}$$

Futhermore, we adopt $< v_{\rm d\text{-}d} >=< v_{\rm d\text{-}d} >_t$, so that this expression is nearly independent of the dust radius $r_{\rm d}$ for ${\rm St} > 1$. For ${\rm St} \gg 1$, the lift-drag ratio approaches asymptotically to a maximum,

$$R_{\rm LD} \simeq 20 \alpha^{1/2} R_1^{-17/8}, \tag{49}$$

where we take the MMSN disk parameters.

We see from Figure 2 that when $r_{\rm d} \sim 10^2$ cm at $R_1 \sim 1$, which corresponds to $g_{\rm D} = {\rm St}^{-1} \sim 0.1$, then the conditions that $t_{\rm col} \sim t_{\rm spindown}$ and that the drag force is represented with the Stokes law are marginally satisfied. In this case, we find $R_{\rm LD} \sim 2.0$ when $\alpha = 0.01$, using Equation (49). Thus, from Figure 4 we obtain $< w_{\rm rel} > \sim 0.1$, which means that the averaged relative velocity due to the lift force is a tenth of $\eta v_{\rm K}$ for the one-meter sized dust at 1 AU from the central star.

4.2 Dependence of the relative velocity on disk parameters

The situation stated in the previous subsection can be qualitatively or quantitatively changed by adopting disk parameters different from MMSN. If we take larger $f_{\rm d}$ than 0.01, as proposed in [8, 17], the averaged relative velocity $< w_{\rm rel} >$ can be ~ 1. The dust to gas ratio $f_{\rm d}$ is included just in the expression of $t_{\rm col}$ (Equation 16), so that larger $f_{\rm d}$ means smaller $t_{\rm col}$ and thereby smaller $r_{\rm d}$ satisfying $t_{\rm col} = t_{\rm spindown}$. This implies that the red line in Figure 2 moves down and that the blue region expands inside. When $f_{\rm d} \sim 0.1$, the blue region includes the dotted magenta line, which shows the grain size satisfying ${\rm St} = 1$, at $R_1 \sim 0.5$. Since $R_{\rm LD} \sim 1$ when $\alpha = 10^{-4}$, we find from Figure 4 that the relative velocity $< w_{\rm rel} > \sim 1$. In this case, the relative velocity due to the lift force $\eta v_{\rm K} < w_{\rm rel} > \sim 60$ m s^{-1}, where we note that $\eta v_{\rm K}$ does not depend on R_1 when $p = 1/4$, exceeds that due to the turbulence $< v_{\rm d\text{-}d} >_t \sim 8$ m s^{-1}, which is computed with Equation (15). Therefore, the lift force is expected to efficiently affect the growth rate of the grain whose size is 10 cm at $R_1 \sim 0.5$ if there is a grain-concentrated part.

Recently, the steeper density profile, which is denser at 1 AU, has been proposed [6]. When the density profile is steeper, a larger q is adopted. If q is larger, the radial profile of the minimum and maximum sizes of the grains is steeper (Equation 23 and dashed green lines in Figure 2). On the other hand, we can find that the red line in Figure 2 does not change as much as the green lines, by comparing Equation (16) to (20). Thus, the blue region in Figure 2 slightly shifts to inner region. Therefore, we expect that when the density profile is steeper with the normalization coefficient fixed, the innermost radius where the lift force continues to be exerted on the grains slightly decreases to get close to $R_1 = 1$.

Suppose that the disk has larger surface density. Spin-down time (Equation 20) and Stokes number (Equation 14) are independent of the surface density Σ_0. On the other hand, collision time is inversely proportional to Σ_0 (Equation 16), so that $r_{\rm d}$ satisfying $t_{\rm col} = t_{\rm spindown}$ is proportional to $\Sigma_0^{-1/2}$ for ${\rm St} \gg 1$. In contrast, $r_{\rm d,min}$ and $r_{\rm d,max}$ in Equation (23) are inversely proportional to Σ_0. Therefore, the blue region moves outside and the mininum grain size in the blue region is nearly-unchanged. The ratio $R_{\rm LD}$ becomes smaller with decreasing R_1, so that the relative velocity due to the lift force is smaller than that for the fiducial surface density.

4.3 Other effects for the model refinement

We can refine the model in this paper by taking into account realistic porosity and shape of the dust grain [19]. If the grain is fluffy, $\rho_{\rm int}$ is smaller than the value we use in Section 2. Equations (14, 18, 17) lead to the dependence of $t_{\rm col}$ on $\rho_{\rm int}$,

$$t_{\rm col} \propto \begin{cases} \rho_{\rm int}^{\frac{1}{2}} & \text{for } {\rm St} \gg 1 \\ \rho_{\rm int}^{0} & \text{for } {\rm St} \ll 1, \end{cases} \tag{50}$$

while $t_{\rm spindown} \propto \rho_{\rm int}^{1}$. Thus, when $\rho_{\rm int}$ decreases, $t_{\rm spindown}$ decreases more rapidly than $t_{\rm col}$, which means that the lift force is exerted on the grain in shorter time. If the grain is lumpy, the coefficient of lift would become as large as a baseball or a golf ball.

It is also worth taking into account realistic collision processes between the grains such as simple scattering (bouncing), minor merger and destruction. Through the simple scattering, the grain may gain the spin angular momentum by means of the surface friction, where the maximum surface velocity of the scattered grains is $v_{\rm d\text{-}d}$, which is less than the mean surface velocity in the case of the major merger (Equation 47). In addition, in the case of a minor merger, which is realized when we consider the size distribution of grains [21], the grains obtain less spin angular momentum compared to the case of the major merger. Thus, we expect less mean relative velocity when the grains undergo the scattering and minor merger. On the other hand, if the destruction (fragmentation) occurs when the grains collide, the grains may gain larger spin angular momentum. The experiments show that agglomerates (cm to dm size) are divided into many fragments that are of mm to cm size through the low-velocity collision [5, 15]. If these fragments have a large spin angular momentum, they can be sufficiently affected by the lift force. How much spin angular momentum grains gain depends on many parameters, so that we defer it to the future work.

The z-component of the lift force, which is omitted in this paper, may affect the resultant relative velocity of the dust grain. The equation of motion in the z-direction includes the gravitational force by the central star, the drag force and the lift force. Although the steady state cannot be realized, because the gravitational force depends on the altitude from the disk mid-plane, the dust grains should gain a momentum in the z-direction. This causes an increase in the absolute value of the velocity, which may result in an increase in relative velocity.

5 Conclusion

In this paper, we investigate the effects of the lift force on the dust grains in the protoplanetary disk from two perspectives. We first investigate whether the lift force is kept exerted on the grains or not. We assume the grains are in the minimum mass solar nebula where the turbulence is developed. We estimate the collision timescale and the spin-down timescale and find that the grain keeps spinning due to the collision with the other grains if the radius of the grain is larger than 100 cm at $\gtrsim 1$ AU from the central star.

We next calculate the mean relative velocity between the grains caused by the lift force. The grains obtain spin angular momenta with various directions by the collision between themselves, so that the lift forces exerted on them have the various directions. Thus, the relative velocity yields between the grains. We assume that the grains are in the steady state and that the distribution of their spin momenta shows the isotropy. We show that the mean relative velocity is comparable to the gas velocity at the Kepler rotational frame, when $F_{\rm L} \gtrsim F_{\rm D}$ and $t_{\rm s} \sim 1/\Omega_{\rm K}$, where $F_{\rm L}, F_{\rm D}, t_{\rm s}$ and $\Omega_{\rm K}$ are the lift force, the drag force, the stopping time of the grains by the drag, and the Kepler angular velocity, respectively. This means that the lift force can sufficiently affect the collision rate, which affects the growth rate of the grains, under the parameter set.

We also estimate the mean relative velocity when the grains keep spinning by combining the above two results. We obtain the result that for the minimun mass solar nebula the mean relative velocity due to the lift force is smaller than the gas velocity at the Kepler rotational frame. We discuss the mean relative velocity as being comparable to the gas velocity if the disk has grain-concentrated parts where the dust-gas ratio is ten times larger than MMSN, so the lift force may affect the collision rate in the parts.

Acknowledgements

M. S. Y. and S. S. K. would thank T. Tsuribe, S. Inutsuka and S. Okuzumi for useful discussions and comments and acknowledge the anonymous referees for useful comments. S. S. K. is supported by a Grant-in-Aid for JSPS Research Fellowships for Young Scientists (A2517840).

Author details

[1]National Astronomical Observatory, 2-21-1 Osawa, Mitaka, Tokyo, Japan. [2]Department of Earth and Space Science, Graduate School of Science, Osaka University, 1-1 Machikaneyama, Toyonaka, Osaka, Japan.

References

1. Adachi, I., Hayashi, C., Nakazawa, K.: The gas drag effect on the elliptical motion of a solid body in the primordial solar nebula. Prog. Theor. Phys. **56**, 1756–1771 (1976)
2. Balbus, S.A., Hawley, J.F., A powerful local shear instability in weakly magnetized disks. I - Linear analysis. II - Nonlinear evolution. ApJ **376**, 214–233 (1976)
3. Birnstiel, T., Dullemond, C.P., Brauer, F., Gas- and dust evolution in protoplanetary disks. A&A **513**, 79–99 (2010)
4. Brauer, F., Dullemond, C.P., Henning, Th., Planetesimal formation near the snow line in MRI-driven turbulent protoplanetary disks. A&A **487**, 1–4 (2008)
5. Deckers, J., Teiser, J., Colliding Decimeter Dust. ApJ **769**, 151–156 (2012)
6. Desch, S.J., Mass Distribution and Planet Formation in the Solar Nebula. ApJ **671**, 878–893 (2007)
7. Goldreich, P., Ward, W., The Formation of Planetesimals. ApJ **183**, 1051–1062 (1973)
8. Hasegawa, Y., Tsuribe, T., Kelvin-Helmholtz instabilities in multi-sized dust layers. PASJ **66**, L2(2014)
9. Hayashi, C., Structure of the Solar Nebula, Growth and Decay of Magnetic Fields and Effects of Magnetic and Turbulent Viscosities on the Nebula. Prog. Theor. Phys. **Suppl 70**, 35–53 (1981)
10. Kataoka, A., Tanaka, H., Okuzumi, S., Wada, K., Fluffy dust forms icy planetesimals by static compression. A&A **557**, L4 (2013)
11. Okuzumi, S., Tanaka, H., Kobayashi, H., Wada, K., Rapid Coagulation of Porous Dust Aggregates outside the Snow Line: A Pathway to Successful Icy Planetesimal Formation. ApJ **752**, 106–123 (2012)

12. Ormel, C.W., Cuzzi, J.N., Closed-form expressions for particle relative velocities induced by turbulence. A&A **466**, 413–420 (2007)
13. Rubinow, S.I., Keller, J.B., The transverse force on a spinning sphere moving in a viscous fluid. J. Fluid Mech. **11**, 447–459 (1961)
14. Sano, T., Miyama, S.M., Umebayashi, T., Nakano, T., Magnetorotational Instability in Protoplanetary Disks. II. Ionization State and Unstable Regions. ApJ **543**, 486–501 (2000)
15. Schräpler, R., Blum, J., Seizinger, A., Kley, W., The Physics of Protoplanetesimal Dust Agglomerates. VII. The Low-velocity Collision Behavior of Large Dust Agglomerates. ApJ **758**, 35–43 (2012)
16. Sekiya, M., Gravitational instabilities in a dust-gas layer and formation of planetesimals in the solar nebula. Prog. Theor. Phys. **69**, 1116–1130 (1983)
17. Sekiya, M., Quasi-Equilibrium Density Distributions of Small Dust Aggregations in the Solar Nebula. Icarus **133**, 298–309 (1998)
18. Shirayama, S., Flow Past a Sphere: Topological Transitions of the Vorticity Field. AIAA Journal **30**, 349–358 (1992)
19. Suyama, T., Wada, K., Tanaka, H., Numerical Simulation of Density Evolution of Dust Aggregates in Protoplanetary Disks. I. Head-on Collisions. ApJ **684**, 1310–1322 (2008)
20. Takagi, H., On the Slow Motion of a Sphere in a Viscous Fluid. J. Phys. Soc. Japan **37**, 505–510 (1974)
21. Windmark, F., Birnstiel, T., Güttler, C., Blum, J., Dullemond, C.P., Henning, Th., Planetesimal formation by sweep-up: how the bouncing barrier can be beneficial to growth. A&A **540**, 73–89 (2012)
22. Youdin, A.N., Goodman, J., Streaming Instabilities in Protoplanetary Disks. ApJ **620**, 459–469 (2005)